STUDIES OF INTERNAL DISPLACEMENTS IN SOLID PROPELLANT GRAINS

(Longitudinal Displacements in Free-Standing, Solid Propellant Hollow Cylinders)

L. U. Rastrelli
R. C. DeHart

INTERIM REPORT
Project 1043-3
Contract Nr. NOnr-3363(00)(FBM)
Nr. 064-451/12-7-61

for

Structural Mechanics Branch
Office of Naval Research
Washington 25, D.C.

1 March 1963

SOUTHWEST RESEARCH INSTITUTE
SAN ANTONIO, TEXAS

(5) 818 600.

SOUTHWEST RESEARCH INSTITUTE
8500 Culebra Road San Antonio 6, Texas

Department of Structural Research

(4)

STUDIES OF INTERNAL DISPLACEMENTS IN SOLID PROPELLANT GRAINS,

(Longitudinal Displacements in Free-Standing, Solid Propellant Hollow Cylinders)

(10) by L. U. Rastrelli and R. C. DeHart,

(9) INTERIM REPORT

(16) Project 1043-3

(15) Contract [redacted], NOnr 3363(00)(FBM)
Nr. 064-451/12-7-61

for

Structural Mechanics Branch
Office of Naval Research
Washington 25, D.C.

(11) 1 Mar[redacted]63,

APPROVED:

Robert C DeHart

Robert C. DeHart, Director
Department of Structural Research

An X-ray scintillation facility was used.

I. INTRODUCTION

The purpose of the tests conducted in this phase of the program was to study the manner in which the sub-surface material in a viscoelastic, thick-walled cylinder deforms with time while subjected to relatively simple mechanical loadings. Measurements of internal displacements were acquired for two, free-standing, solid propellant models. Each model was subjected to a mechanical loading consisting of either a sustained uniaxial compression or a combination of sustained uniaxial compression and internal pressure.

II. DESCRIPTION OF TEST SPECIMENS AND PROCEDURES

The X-ray scintillation detection facility used for determining the location of embedded and surface particles is described in Reference 1. The nomenclature for spatially identifying the particles, and the procedures for measuring particle movements and for computing the displacements are given in Appendix B, Reference 2. Confidence limits for the displacement data were developed in accordance with the procedures described in Appendix A, Reference 2 and in Reference 3.

The propellant formulation used was that of a representative, composite propellant containing (by weight) approximately 80% solids. The two hollow cylinders used in the tests reported herein were from the same batch of solid propellant. One of the grain models (S 20) was continuously cast; small, lead pellets were introduced during various stages of curing. The resulting random array of embedded particles were subsequently located spatially (i. e., in terms of cylindrical coordinates) radiographically. The final test article (including the post-cure, surface-mounted particles) is shown in Figure 1. The other model grain (S 21) was segmentally cast in order to preposition the embedded particles (see Figure 1).

Experience from previous tests indicated that the displacements under constant-load conditions and during the subsequent, post-load recovery period were extremely time-dependent. Since acquiring a trace for each particle (both embedded and surface-mounted) could result in a distorted and discontinuous displacement history, it was deemed advisable to arrange the X-ray scanning schedule so that selected embedded particles would be monitored continuously with only infrequent check-scans of the surface particles.

For Model S 20, an embedded particle as close to the cylinder's midlength as possible (in this case, particle 412) was selected for continuous observation. The scanning procedure entailed the acquisition of longitudinal traces containing the top and bottom (stationary) load platens and the midlength particle. Three embedded particles (411, 511, 611) were used for Model S 21. Longitudinal traces were acquired by scanning along the cylinder element (r = 1) containing these embedded particles.

The original objective of this phase of the program was to acquire measurements of the radial displacements (both sub-surface and surface) for a hollow cylinder subjected to a sustained internal pressure. Free-standing (rather than case-bonded) grains were selected on the basis that the rather large and therefore readily

measurable radial deformations would occur. The problem of providing end closures which would, on one hand, permit the application of meaningful internal pressures, and at the same time avoid the complicating boundary conditions and barrelling effects associated with mechanical seals, could apparently be solved by applying a small uniaxial compressive loading to the cylinder's lubricated ends. Previous experience with unfilled urethane models clearly indicated that this technique was indeed feasible for internal pressures up to 20 psi. By carefully controlling the load platen and cylinder ends' finish, the uniaxial compressive load would be of secondary importance and would serve primarily as a means of seating and sealing the lubricated ends of the grain.

However, it became apparent in preliminary tests of filled grains that the axial loads required to produce an effective seal for meaningful internal pressures would have to be of such magnitudes as to induce creep phenomena (as indicated by measurements of overall cylinder lengths). In essence, then, it was quite probable that in any test involving a combined uniaxial compression-internal pressure loading, the measured internal displacements would reflect not only the quasi-static effects but also the creep induced by either or both types of loadings. The data would then depict rather complex

inter-related, time-dependent deformation behavior which could obscure and leave undetected a rather basic, internal displacement phenomenon.

Nevertheless, it was felt that much could be gained by subjecting at least one model to a uniaxial compression-internal pressure sequential loading. The internal displacement data acquired would undoubtedly uncover significant (and heretofore unknown) deformational trends and at the same time, provide information which would be useful in subsequent model tests.

With this in mind, Model S 20 was subjected to the initial load sequence shown at the bottom of Figure 2 consisting of a sustained, uniaxial compression loading of 26 psi with shorter-duration excursions of 5 and 12 psi internal pressure. This was followed by a rather prolonged zero-load period during which time measurements were made of the model's recovery. The uniaxial compression loading was then reapplied, followed rather closely by the application of 15 psi internal pressure. Both types of loads were maintained for approximately 24 hours, and then removed.

The displacement data acquired from Model S 20 indicated that the uniaxial compressive loading in Phase A overshadowed the effects produced by the internal pressures. This, in turn, suggested that it

might be advisable to limit the initial loading on Model S 21 to uniaxial compression whose magnitude (26 psi), duration (some 48 hours) and subsequent recovery period (approximately 32 days) would be the same as that used for Model S 20. In so doing, it would be possible to acquire a better understanding of the creep and recovery phenomena. Unfortunately, a failure in the compressed air system for pneumatic loading device caused the load to be removed prematurely (see Figure 3). This, in turn, shortened the recovery period considerably since all the measured displacements stabilized in approximately 4 days (in contrast to the 32 days required for Model S 20). The combined uniaxial compression-internal pressure in Phase B duplicated (in magnitude) the final loadings experienced by Model S 20. The duration (which was slightly less) was governed by the time required for the displacements to stabilize.

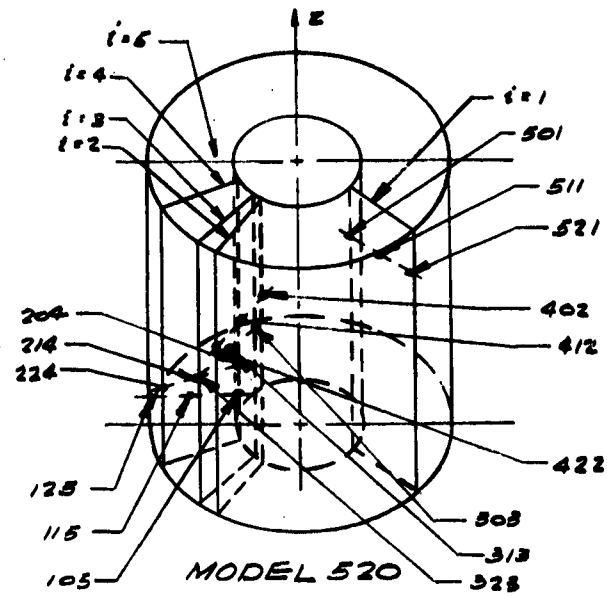

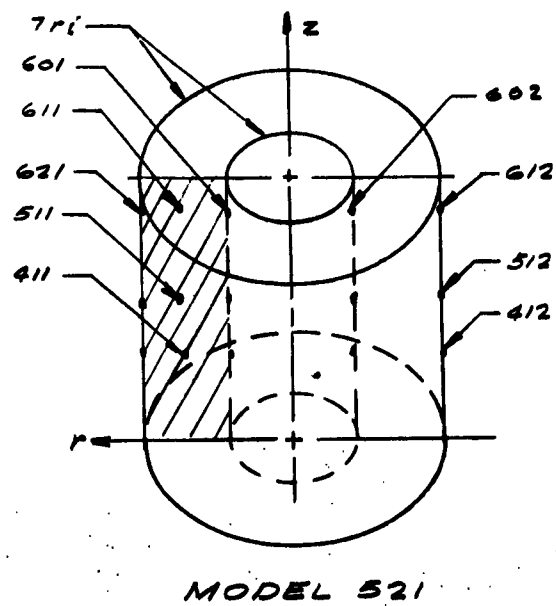

FIGURE 1. Location of Embedded Particle in Solid Propellant Models S 20 and S 21

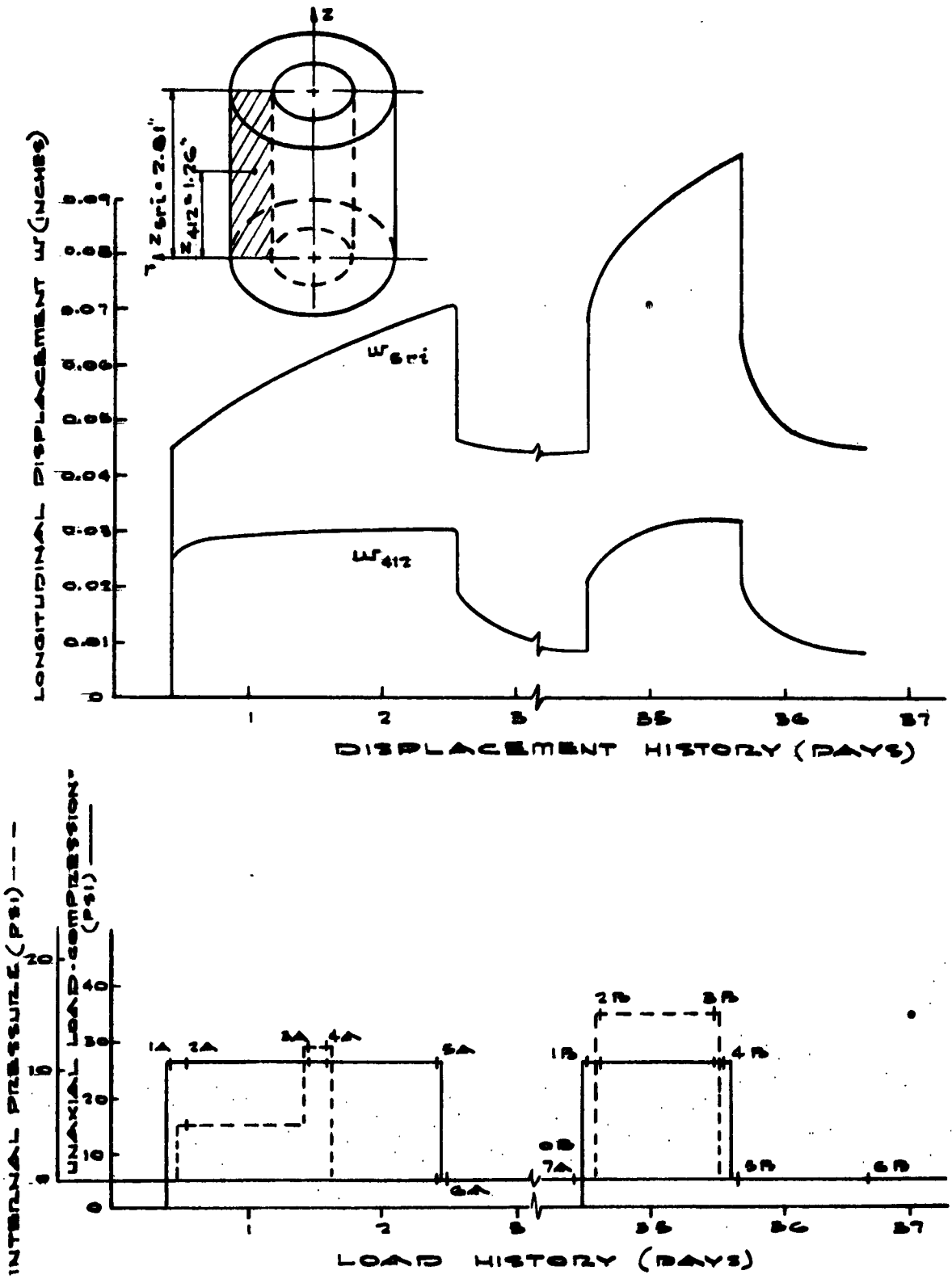

FIGURE 2. Load and Longitudinal Displacement Chronology for Model S 20

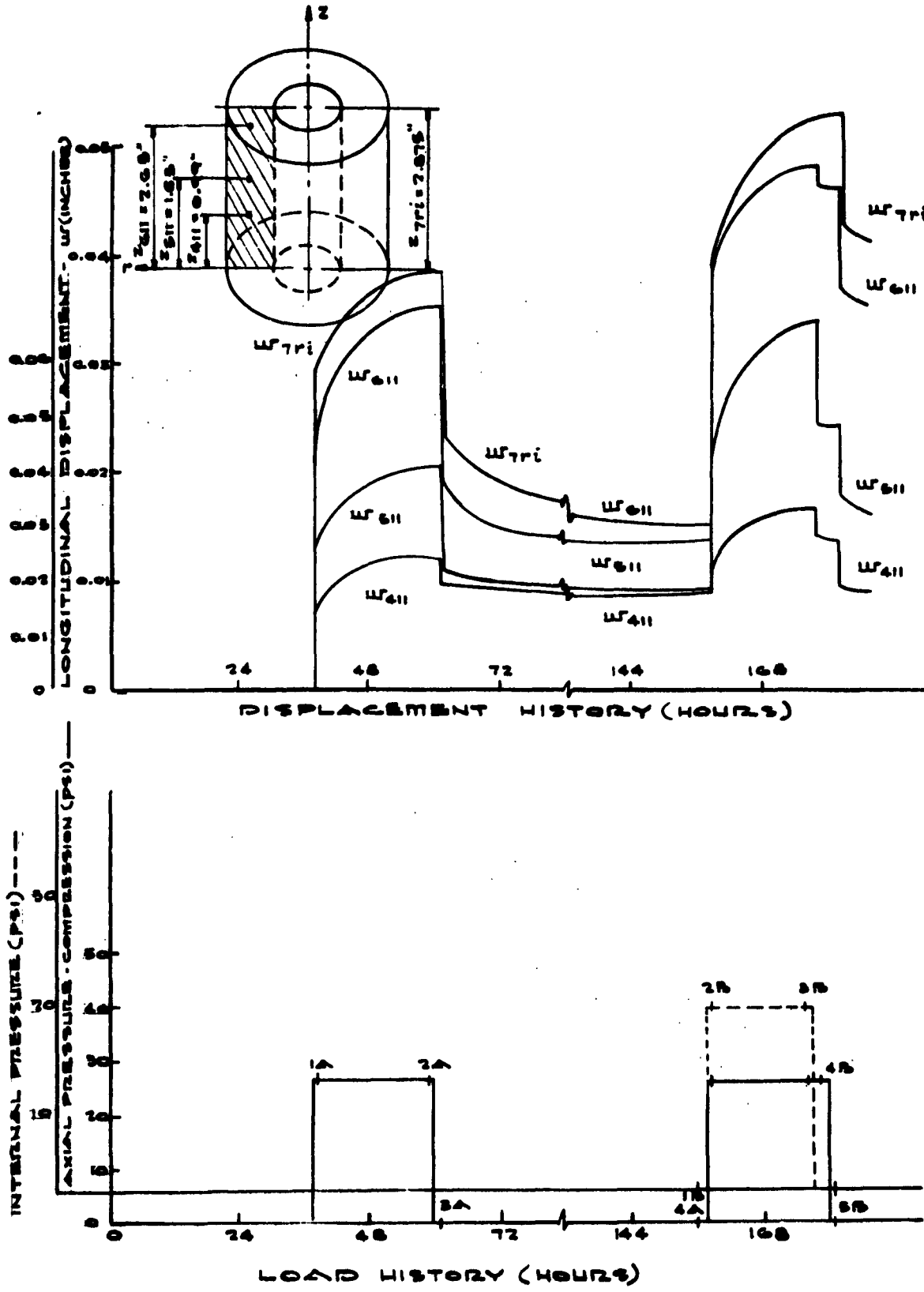

FIGURE 3. Load and Longitudinal Displacement Chronology for Model S 21

III. DISCUSSION OF RESULTS AND CONCLUSIONS

At the top of Figures 2 and 3 are curves depicting the chronological variation of the platen-to-platen (or overall) longitudinal displacements and the longitudinal displacements for one or more points within the cylindrical models.

The overall longitudinal displacements (as acquired by measuring the change in position of the movable, top load platen) represents the type of data that would be normally obtained in the usual compression tests. Of particular interest for Model S 20 was whether or not the displacement experienced by the embedded, mid-length particle deviated in some unpredictable fashion from that indicated by the more common, overall displacements.

From the uppermost, overall displacement curve at the top of Figure 2, it is apparent that the cylinder exhibits the following characteristics: (a) a continuous, longitudinal shortening which is apparently unaffected by internal pressurization; (b) a subsequent initial recovery which is nearly equal to the total accumulated creep; (c) essentially a zero post-load recovery resulting in a residual displacement whose magnitude is nearly equal to pre-creep phase displacements; (d) upon reapplying the uniaxial compression

and internal pressure loadings, the overall displacement clearly reflects the cylinder's prior load experience; and (e) a subsequent, post-load recovery which results in a residual displacement roughly equal to that present at the end of the initial loadings.

All in all, it may be said that although the overall displacement curve exhibits some rather unique quantitative features with regard to the creep and recovery associated with two cycles of intermittent loadings, there is nothing of a qualitative nature which is particularly remarkable. The same statement could, in a broad sense, be made with regard to the embedded, mid-length particle displacement w_{412}. However, when the two curves are compared, it is apparent that the point within the grain displaces in a fashion which is only remotely similar to that indicated by measurements of the platen-to-platen distance. For example, the creep rate, creep accumulation, initial recovery and post-load recovery rates and magnitude for the internal point are all different than those found by the overall measurements. Moreover, during the second loading (Phase B) the embedded particle did not exhibit the pronounced accumulative effect found for the overall displacement.

The longitudinal displacement data acquired for Model S 21 display the same general characteristics. During the initial, uniaxial

compression loading and the subsequent post-load recovery period, the amount of longitudinal creep and recovery experienced by the two embedded particles near the cylinder's mid-length (411 and 511) was clearly quite different than that of an embedded point near the top platen (611) and the top platen, itself. The displacements acquired during the Phase B loading (combined uniaxial compression and internal pressure) exhibited trends that were unique with respect to not only the Phase B displacements acquired for Model S 20 under similar load circumstances, but also with respect to the prior Phase A loading. In particular, there is the fact that while the overall displacement did not reflect the removal of the internal pressure, the internal particle (including 611) did indeed instantaneously and erratically decrease.

Aside from the readily apparent and rather general conclusion that the amount that a point within the cylinder displaces is quite different than that indicated by the overall longitudinal displacement, there are other indications that are noteworthy. For example, it is obvious that the creep and recovery experienced by the internal particles are in some presently unknown fashion not only time but also spatially dependent. The limited experimental evidence (coupled with a lack of any prior internal displacement

experience upon which to base a hypothesis) does not lend itself to the development of a clear rational mathematical statement which would, for example, link the overall and internal displacements. There are, however, some rather vague qualitative trends which would seem to indicate that similar tests involving a simpler material (say, unfilled urethane) under uniaxial compression or tension (with no complicating internal pressurization effects) could uncover some rather basic phenomena that would point the way to a governing law.

REFERENCES

1. Rastrelli, L.U. and DeHart, R.C., "Studies of Internal Displacements in Solid Propellant Grains (Embedded Particle, X-Ray Detection System)", Interim Report, SwRI Project 1043-3, ONR Contract No. Nonr-3363(00)(FBM), 1 Sept. 1962.

2. Rastrelli, L.U. and DeHart, R.C., "Studies of Internal Displacements in Solid Propellant Grains (Displacements in Cylindrical Unfilled-Urethane Specimens under Uniaxial Compression)", Interim Report, SwRI Project 1043-3, ONR Contract No. Nonr-3363(00)(FBM), 1 Oct. 1962

3. Rastrelli, L.U. and Pape, B.J., "Studies of Internal Displacements in Solid Propellant Grains (Estimating Errors in X-Ray Detection Facility)", Interim Report, SwRI Project 1043-3, ONR Contract No. Nonr-3363(00)(FBM), 5 Sept. 1962.